Per-*O*-methylated α- and β-CD: Cyclodextrins with Inverse Hydrophobicity[1]

Stefan Immel and Frieder W. Lichtenthaler, Darmstadt (Germany)

The investigation focuses on the computer-aided generation of the molecular geometries, contact surfaces, and lipophilicity patterns of per-*O*-methylated α-CD (**1**) and its β-CD homolog **2**, and compares them with their parent non-substituted cyclodextrins. The molecular geometries, compared via statistical analysis of crystal structure data available, reveal **1** and **2** to be considerably more flexible than α- and β-CD, allowing wide variations in the tilting of the glucose units relative to the macrocyclic ring axes. The comparative evaluation of their contact surfaces not only discloses a substantial increase of the torus heights upon per-*O*-methylation (from ≈8.0Å in α- and β-CD, to ≈11.1Å in **1** and **2**), but also an enlargement of their cavity areas by 40% (+35Å^2 for α-CD → **1**) and 70% (+75Å^2 for β-CD → **2**), respectively. The hydrophobic characteristics of **1** and **2**, emerging from the *m*olecular *l*ipophilicity *p*atterns (MLPs) generated and projected onto the contact surfaces in color-coded form, are inverse to those for α- and β-CD: the most hydrophobic surface regions of **1** and **2** are located at the torus rims made up by the 2-OMe and 3-OMe groups at one side, and the 6-CH_2OMe moieties at the other, with a hydrophobic "band" wrapping around the outside of the macrocycles; these "exo-lipophilic" topographies are opposed by pronouncedly hydrophilic central cavities. A variety of experimental findings can be rationalized on the basis of the opposite lipophilicity profiles of the CDs and their permethylated analogs, such as for example the opposite orientation of benzaldehyde, *p*-nitrophenol, and 3-iodopropionic acid in the cavities of α-CD and of **1**. Thus, the notion is substantiated that the operation of dispersive interactions between guest and CD-host cavities play a more dominant role in inclusion complex formation than hitherto appreciated.

Per-*O*-methyliertes α- und β-CD: Cyclodextrine mit inverser Hydrophobie. Vorliegende Arbeit befaßt sich mit der Computer-unterstützten Generierung der molekularen Geometrien, der Kontaktoberflächen und der Lipophilie-Profile von per-*O*-methyliertem α-CD (**1**) und seinem β-CD Homologen **2**, und vergleicht diese mit den für α-CD und β-CD erhaltenen Daten. Der Vergleich molekularer Geometrien auf der Basis einer statistischen Analyse verfügbarer Kristallstruktur-Daten zeigt eine deutlich höhere Flexibilität von **1** und **2** gegenüber den zugrundeliegenden Cyclodextrinen, insbesondere hinsichtlich der Variabilität der Schrägstellung der Glucose-Einheiten relativ zur Ringachse der Macrozyklen. Eine vergleichende Bewertung der Kontaktoberfläche zeigt nicht nur ein deutliches Ansteigen der Torushöhe durch per-*O*-methylierung (von ≈8.0Å in α- und β-CD auf ≈11.0Å in **1** und **2**), sondern auch eine Vergrößerung der Hohlraum-Oberfläche um 40% (+35Å^2 beim Übergang von α-CD → **1**) und 70% (+75Å^2 für β-CD → **2**). Die Verteilung hydrophiler und hydrophober Oberflächenregionen in **1** und **2** – wie sie sich aus den in Farbkodierung auf die Kontaktoberfläche projizierten MLPs (*M*olecular *L*ipophilicity *P*atterns) ergibt – ist invers zu der in α- und β-CD vorliegenden Situation: beide Torusränder, d.i. die 2-OMe/3-OMe Seite ebenso wie der gegenüberliegende 6-CH_2OMe Rand stellen Zonen höchster Hydrophobie dar, während die Außenseiten der Makrozyklen durch ein gemischt hydrophil/hydrophob durchsetztes Band charakterisiert sind; diesen "exo-lipophilen" Topographien steht eine ausgesprochen hydrophile Hohlraumregion gegenüber. Das Wissen um die entgegengesetzten Lipophilie-Profile von Cyclodextrinen und ihrer permethylierten Derivate läßt eine Reihe experimenteller Befunde verständlich erscheinen, so z.B. die jeweils umgekehrte Einlagerung von Benzaldehyd, *p*-Nitrophenol und 3-Jodpropionsäure in α-CD und **1**. Dies erhärtet die Vorstellung, daß dispersive Wechselwirkungen zwischen Gast und CD-Wirt eine dominantere Rolle bei der Bildung von Einschlußkomplexen spielen als bislang angenommen.

1 Introduction

Ample evidence has accumulated that the cyclodextrins are truncated cone structures with hydrophilic exteriors and hydrophobic inner cavities, lined largely by H-3 and H-5 of the glucose units and their intersaccharidic oxygens, which together generate a distinctly hydrophobic environment. These unique features enable them to form inclusion complexes with a large variety of organic and inorganic compounds [2, 3].

Whilst the term hydrophobicity is as yet quite elusive to exact experimental characterization [4], it yields to computer modeling, which provides a particularly lucid picture in the case of the cyclodextrins [5, 6] and their inclusion compounds [7]. Thus, the hydrophobic topographies of α-, β-, γ-, and δ-cyclodextrin have been portrayed on the basis of their computer-generated **m**olecular **l**ipophilicity **p**atterns (**MLP**s), as projected onto their solvent-accessible contact surfaces. These MLP patterns of the cyclodextrins reveal the 2-OH/3-OH sides of the macrocycles, i.e. the respective wider torus rim, to be distinctly hydrophilic, whereas the opposite narrower opening, made up of six to nine CH_2OH groups, is intensely hydrophobic, yet the surface regions of highest hydrophobicity reach from there well into the respective cavities [6].

Any chemical modification of the native cyclodextrins – be it *O*-substitution [8], replacement of hydroxyl groups against hydrogen, halogen, *N*-, or *S*-substituents [8], or exchange of the glucose moieties by other sugars such as mannose [5, 9], altrose [10], or galactose [5] – is apt to alter the distribution of hydrophilic and hydrophobic surface regions substantially. To expound on a few, uniformly substituted cases: the all-6-deoxy derivatives of α-, β-, and γ-CD, prepared by replacement of the primary 6-OH groups with hydrogen [11], are surmised to have distinctly enlarged hydrophobic surface areas on the narrower rim side; the same would be expected in an even more pronounced form for the respective per-6-bromo-[11], per-6-iodo-[12], or per-6-azido cyclodextrins-[13]. Unfortunately, their complexation properties, that are undoubtedly different from those of the parent cyclodextrins, have yet not been studied in detail. However, the observation that per-6-azido-β-CD forms face-to-face hydrogen-bonded dimers in the solid-state [14] – as contrasted to β-CD, which packs with 12 water molecules in a monomeric herringbone-type structure [15] – gives some indication as to the altered lipophilicity profiles. These are also reflected by the finding [16] that per-6-bromo- and per-6-azido-cyclodextrins form molecular layers at the air-water interface, in which the organized structures closely resemble those of the compounds in the solid-state.

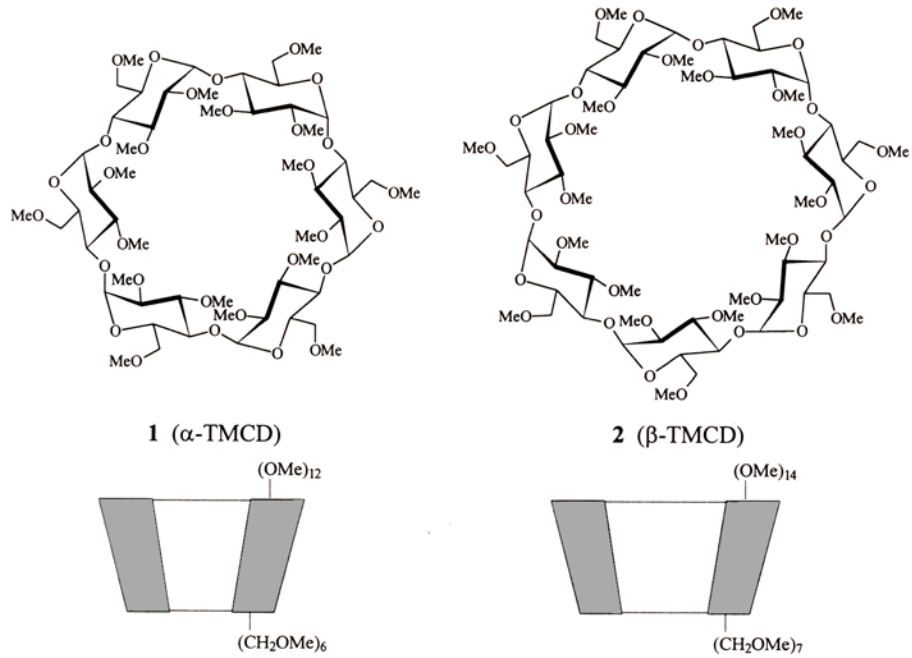

Figure 1. Formulae and schematic representations of the per-*O*-methylated α- and β-cyclodextrins, α-TMCD (**1**) and β-TMCD (**2**).

More profound changes in the allocation of hydrophobic and hydrophilic surface regions of the cyclodextrins are surmised to result from functionalizations on the 2-OH/3-OH side, i.e. the wider opening of the truncated cone structures. This secondary OH-face is markedly hydrophilic (cf. MLPs in ref. [6]), and should – on deoxygenation, *O*-acylation, or *O*-alkylation – eventually permute to hydrophobic surface areas.

A most comprehensive permutation of hydrophilic against hydrophobic surface regions is expected to be effected by per-*O*-acylation or per-*O*-alkylation of the cyclodextrins, which is readily achieved experimentally [8]. The per-2,3,6-tri-*O*-methyl derivatives of α-cyclodextrin (α-TMCD, **1**) and of its next higher homolog, β-TMCD (**2**), not only have higher solubilities in organic solvents, but also in water as well, as behavior that is conceivably caused by the non-availability of the intramolecular hydrogen bond network prevailing in the unsubstituted CDs [17]. In addition, the steric hindrance exerted by the 12 resp. 14 secondary methoxy groups on the wider rim of **1** and **2** (cf. Figure 1) results in a sizable increase of the distances between O-2 of one glucose unit and O-3 of the next, entailing a sharper inclination of "glucose-ribbon" towards the 6-CH_2OH opening, and thus rendering the a priori smaller opening of the truncated cone even narrower [18].

As thus the cavity dimensions of per-*O*-methylated cyclodextrins **1** and **2** are different from those of the parent CDs, the guest-host interactions in their inclusion complexes must differ for steric reasons already. As a typical example, the solid-state geometries of the inclusion complexes formed by α-CD and **1** with *p*-iodoaniline [19] not only differ in the depth with which the guest is inserted into the respective cavity (cf. Figure 2), but also by a water molecule being additionally included in the cavity of **1.** More significantly though, the overall orientation mode of the guest in the host cavity can be different: 3-iodopropionic acid [20], benzaldehyde [21], and *p*-nitrophenol [22], for example, are incorporated in opposite arrangements into the cavity fo α-CD and its methylated-derivatives, as illustrated in Figure 2 by cross-cut plots through the respective molecular contact surfaces of the molecular assemblies.

At the root of this contrasting behavior are not only differences in the geometries of the CDs and their permethylated counterparts, but other factors, such as polar (dipole-dipole) and hydrophilic/hydrophobic interactions which, as of now, have not been assessed. As these undoubtedly play a decisive role in the chiral recognition capabilities of alkylated CDs [23, 24], that are substantially improved over those observed for the parent cyclodextrins, we decided to get a first conception on the lipophilic characteristics of **1** and **2** via generation of their molecular lipophilicity patterns (MLPs). This is subject of this paper, a task that was substantially facilitated by the availability of solid-state structural data for many inclusion complexes of **1** and **2** [18], as these provide an excellent starting point for molecular modelling studies.

2 Results and Discussion

2.1 Molecular geometries of per-*O*-methylated α-CD and β-CD

The per-*O*-methylated α-CD (**1**) and β-CD units (**2**), extracted from the crystal structures of the iodoacetic acid monohydrate [20a] and (*S*)-2-(2-fluor-biphen-4-yl)propionic acid [25] inclusion complexes, were chosen as representative examples for comparatively unstrained structures; their molecular geometries, in ball-and-stick representations, and their contact surfaces in the common dotted form are shown in Figure 3. As clearly evident therefrom and the comparative data listed in Table 1, both exhibit unusually wide ranges of glucose tilt angles τ [6] between 91–106° for **1** and 77–128° for **2,** that denote widely variable inclinations of the glucose units relative to the macrocycle. In addition, substantial variations of the atomic distances between intersaccharidic oxygens di-

agonally across the macrocycle (8.24–8.72Å for **1** and 9.26–10.15Å for **2**) are observed, reflecting an asymmetric distortion towards an elliptical shape of the cyclodextrin ring. Accordingly, the macrocycle of the permethylated CDs is more flexible (i.e. more "distortable") than in the unmodified CDs, obviously due to steric hindrance between the methyl groups and the lack of a stabilizing hydrogen bond network at both torus rims. This has been noted previously [17], and was supported by a more recent NMR study [26], indicating that steric bulk introduced by *O*-methylation leads to flattened-shape geometries of the macrocycles in solution, in good agreement with the data derived from X-ray structural data (Table 1).

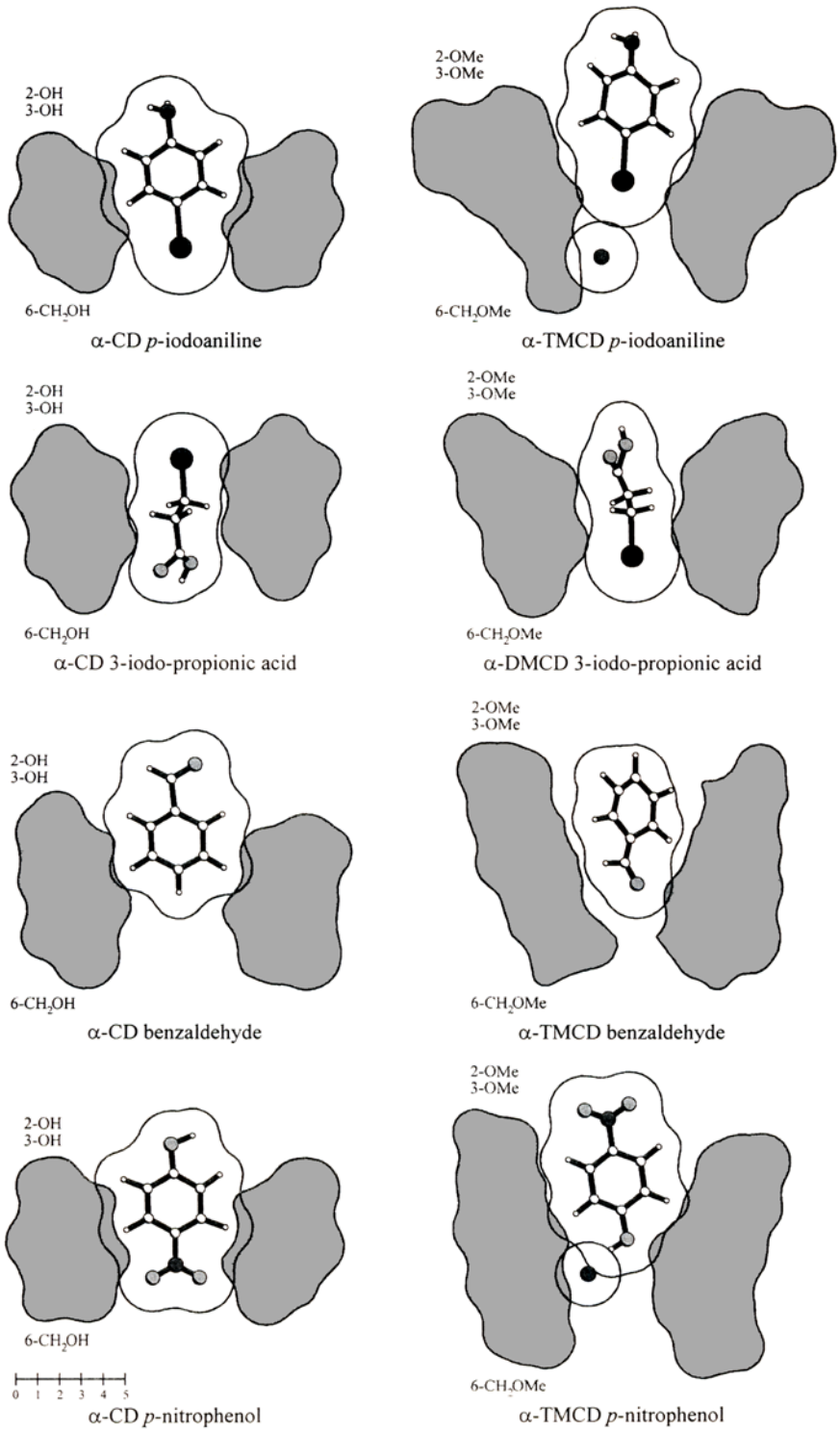

Figure 2. Comparison of typical solid-state inclusion complex geometries of α-CD (left column each) and its per-*O*-methylated derivative **1** (right column, resp.), on the basis of cross-section plots through their contact surfaces, which were sliced through the center of geometry with ball-and-stick models of the guest molecules inserted (for reasons of clarity model insertions of the CD-hosts were omitted). *Top:* p-iodoaniline is imbedded into the α-CD and α-TMCD cavity in the same mode, yet with different depths of immersion due to a water molecule (as indicated by the isolated sphere) in the lower half of the α-TMCD cavity (right); the amino group protruding from the secondary hydroxyl resp. methoxyl face [19]. – *Center and bottom entries:* The immersion mode of 3-iodopropionic acid [20], benzaldehyde [21], and *p*-nitrophenol [22] into the cavity of α-CD (left row) is opposite to that of per-2,6-O-methyl-α-CD and α-TMCD (**1**, at right each).

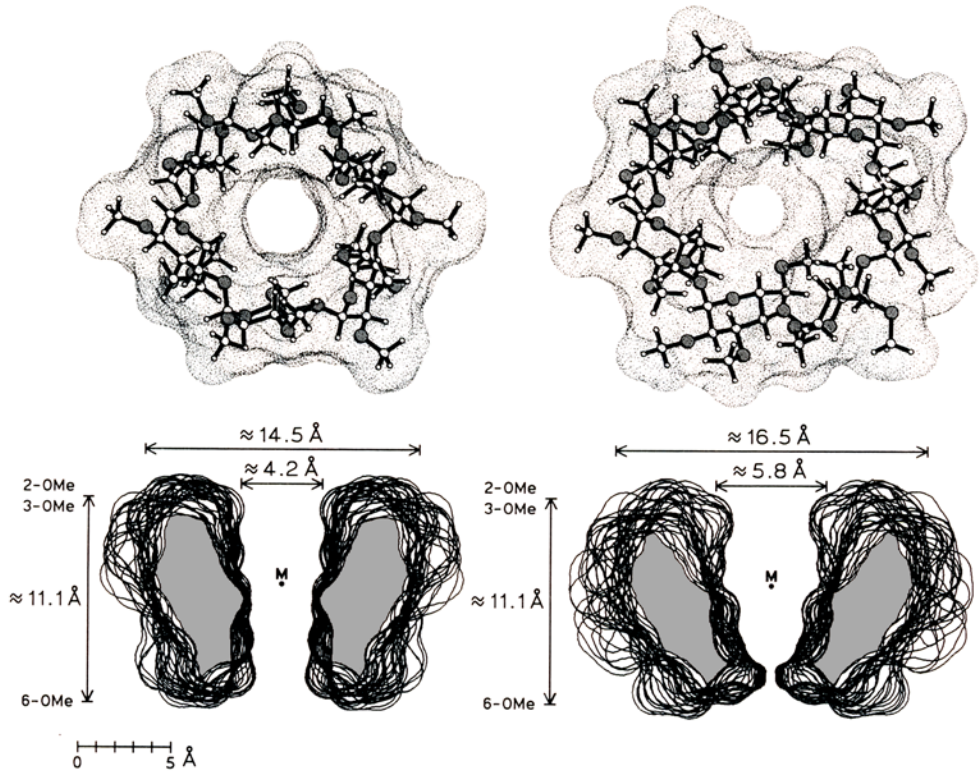

per-2,3,6-*O*-methyl-α-CD
1

per-2,3,6-*O*-methyl-β-CD
2

Figure 3. *Top:* Dotted contact surfaces of representative per-*O*-methyl-α-CD (**1,** left) and per-*O*-methyl-β-CD units (**2,** right), with ball-and-stick models inserted. The molecular geometries were obtained from the solid-state structures of the hexakis(2,3,6-tri-*O*-methyl)-α-cyclodextrin iodoacetic acid monohydrate [20a] and heptakis(2,3,6-tri-*O*-methyl)-β-cyclodextrin (*S*)-2-(2-fluoro-biphen-4-yl)propionic acid [25] inclusion complexes by removal of the guest. The molecular orientation is uniformly such that the 2-OMe and 3-OMe groups are facing the viewer, whereas the 6-CH_2OMe moieties point away from him. – *Bottom:* Side-view cross-section plots through the contact surfaces of **1** and **2,** respectively, with the approximate molecular dimensions being indicated (M: center of geometry).

As typical examples, the per-*O*-methyl CDs **1** and **2,** depicted in Figure 3, exhibit only slightly puckered macrocycles, with average displacements of the O-1 atoms from planarity (i.e. the atomic distances of *each* O-1 atom from the least-squares best-fit mean plane formed by *all* O-1 atoms) of 0.14(5)Å for **1,** and 0.36(18)Å in **2.** Statistical analysis of the geometry parameters found for the intersaccharidic bond and torsion angles in all solid-state structures of α-CD and β-CD, as well as their per-2,6-*O*- and per-2,3,6-*O*-methylated derivatives, reveals only slight changes of the corresponding mean values with increasing ring size (i.e. going from six to seven monosaccharide units, cf. Table 1), or upon the effect exerted by *O*-methylation. The glucose units invariably adopt standard $^4C_1$ chair conformations as evidenced by the *Cremer-Pople* puckering parameters [27] listed in Table 1, with $\theta \approx 0.01-10.0^\circ$ and medium puckering amplitudes of Q≈0.55–0.60Å that are typical for unstrained glucose conformations. The $\Phi(O_5\text{-}C_1\text{-}O_1\text{-}C_{4'})$ torsion exhibits values of around 105–115°, whereas $\psi(C_1\text{-}O_1\text{-}C_{4'}\text{-}C_{3'})$ falls into the 125–135° range. However, the larger root-mean-square (RMS) deviations found for the torsions in the methylated CD-structures indicate an increased flexibility of the macroring, entailing a larger range of different geometries for the intersaccharidic linkages. Most notably, the tilt angles τ [6] indicate an almost perpendicular arrangement of the monosaccharide units relative to the CD ring ($\tau \approx 100-110^\circ$), with the 6-$CH_2$-OR groups invariably being slightly canted towards the molecular center, whilst the 2-OR and 3-OR functions, in all cases, point away from central molecular axis ($\tau > 90^\circ$) [6]. In particular the small RMS-fluctuations found for the glucose tilting in the natural, unsubstituted CDs display their macrorings to be regularly shaped with a high degree of symmetry, whilst the larger fluctuations in **1** and **2** indicate an increased conformational flexibility and a less ordered arrangement of the glucose units (cf. Table 1).

2.2 Contact surfaces and molecular dimensions of per-*O*-methylated cyclodextrins

The contact surfaces of **1** and **2** as shown in Figure 3 (top), lucidly display their effective steric properties and molecular dimensions, whilst the cross-section plots through these surfaces reveal their torus diameters to be slightly larger than those observed for the parent (unmodified) α-CD and β-CD [6] (cf. Table 1). However, comparison of the cavity dimensions shows them to be wider for **1** and **2** at their 2-OMe/3-OMe torus rims, and narrower in the center portions than those observed for α-CD and β-CD. Due to their pronouncedly increased torus heights (≈11.1Å for **1** and **2,** as compared to approximately 8.0Å for α- and β-CD [6]), their cavity volumes are about 10–20% larger (cf. Table 1). In relation to the comparatively large total surface areas (970 and 1130Å^2 for **1** and **2**), the cavities are relatively small, comprising estimated regions of 120 and 180Å^2 only. On the other hand, the surface areas inside the cavities of **1** and **2** are distinctively larger – by 35 and 75Å^2, respectively – than the cor-

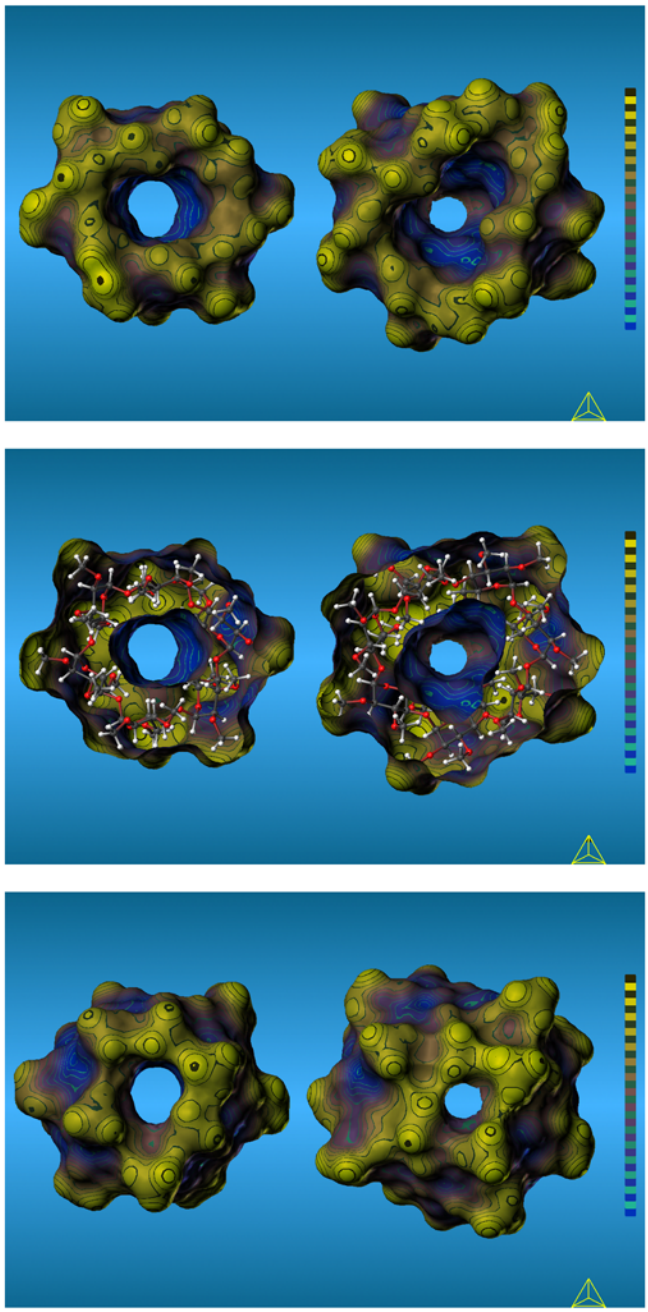

Figure 4. Molecular lipophilicity patterns (MLPs) for the guest-free structures of per-*O*-methyl-α-CD (**1** [20a], left entries) and per-*O*-methyl-β-CD (**2** [25], right resp.) projected onto their contact surfaces of Figure 3 in color-coded form: blue colors designate hydrophilic surface regions, yellow areas correspond to hydrophobic domains. The top picture views through the larger openings of the conically shaped molecules, thus exposing the intensively hydrophobic (yellow) 2-OMe/3-OMe side. In the middle, the front half of the surfaces has been removed to provide an inside view onto the backside; in addition, a ball-and-stick model was inserted to illustrate the molecular orientation. The bottom representation depicts the "backside" of **1** and **2,** i.e. the smaller opening with the 6-CH_2OMe groups facing the viewer (models were rotated by 180° around a vertical axis). Since the color-code applied was adapted to the calculated range of MLP values for each molecule separately, not direct comparisons of the models presented here with those for the parent, unmodified CDs [6] should be made. As, *in toto,* **1** and **2** are much more hydrophobic than α- and β-CD, the coloring only illustrates the relative distributions of most hydrophobic and hydrophilic surface regions for each individual molecule and does not provide scaling in absolute values.

responding surface areas for α-CD and β-CD (cf. Table 1). This at first somewhat surprising finding undoubtetly contributes to the higher capacity of methylated CDs for chromatographic separations in general, and due to their structurally more differentiated cavities, for the separation of enantiomers, in particular.

2.3 Molecular lipophilicity patterns of per-*O*-methylated cyclodextrins

Following the methodology used previously [5–7], the **m**olecular **l**ipophilicity **p**atterns (**MLP**s) for **1** and **2** were generated with *Brickmann*'s MOLCAD program [28], and projected onto the contact surface in color-coded form to facilitate visualization [29]: blue colors correspond to hydrophilic regions (mental association with water), and yellow depicting hydrophobic domains (cf. Figure 4).

From these imposing color-graphics, remarkable differences in the lipophilicity profiles of the α- and β-CD [6] and their permethylated derivatives **1** and **2** become evident: in the former, the wider torus rim carrying the secondary hydroxyl groups, is distinctly hydrophilic, whereas the primary hydroxyl face is characterized by well-defined hydrophobic surface areas reaching into the cavity [6]. In the permethyl-CDs **1** and **2,** this front-/back-side separation of hydrophilic and lipophilic domains has vanished almost completely, as both torus rims are covered by an equally dense layer of methyl groups of very similar hydrophobicities. More lucid in this respect are the side-view models (Figure 5): a hydrophobic surface band wraps around the outside of each of the CD tori, that is opposed by distinctly hydrophilic surfaces regions on the inside of the cavities. Accordingly, the permethyl-CDs **1** and **2,** and by extrapolation, all other per-O-alkylated CD derivatives, may truly be considered as cyclodextrins with "inverse" lipophilicity profiles – a status that must imply far-reaching consequences on their behavior towards incorporation of guest molecules.

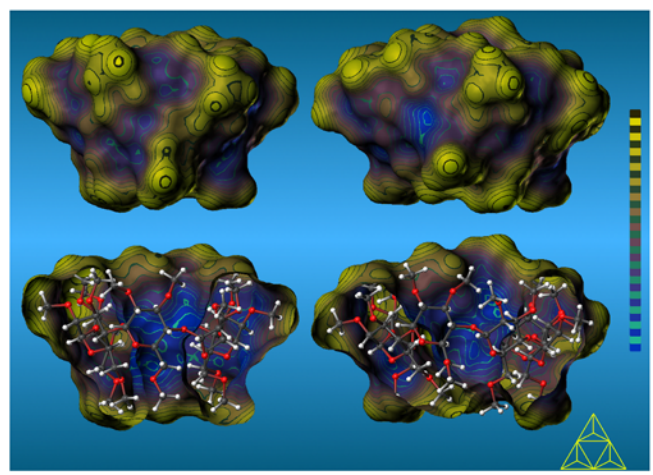

Figure 5. Side-view MLPs, in closed and bisected form each, of the per-*O*-methylated αCD (**1,** left models) and β-CD (**2,** right side each), respectively; color coding according to Figure 4. Their orientation is uniformly such that the 2-OMe/3-OMe side is aligned upward (larger opening of the torus), and the 6-CH_2OMe groups point downward, corresponding to the cross-section plots of Figure 3. The distribution of hydrophilic (blue) and hydrophobic (yellow) surface areas clearly reveals them to be CDs with inverse lipophilic topographies, i.e. pronouncedly hydrophilic cavities versus uniquely mixed outside surfaces with hydrophobic regions being interspersed with hydrophilic ones.

Indeed, a variety of experimental data available may be rationalized on the basis of essentially opposite lipophilicity profiles of CDs and their per-*O*-methylated counter-parts, most notably the opposite orientation of the same guest molecules in the respective cavities: benzaldehyde and *p*-nitrophenol (cf. cross-cut representations in Figure 2) enter the wider cavity side of α-CD with their hydrophobic portions; the hydrophilic sections (-CHO and -OH, respectively) stick out therefrom for better accessibility to solvation by the solvent, or by OH-groups of the host or an adjacent CD in the solid-state. However, in the per-*O*-methyl-α-CD (**1**, cf. Figure 2) – not unexpected on the basis of its hydrophilic cavity – benzaldehyde and *p*-nitrophenol are inversely oriented, i.e. with their hydrophilic, polar groups (-CHO and -OH, resp.) inserted into the cavity.

There are other forms of inclusion complex formation though: in the case of *p*-iodoaniline, the principal orientation of the guest in the cavity of α-CD and α-TMCD (**1**) are the same, insertion occurs from the secondary hydroxyl side with the iodine substituent first. However, the extent of penetration into the cavity is different: the benzene ring being fully immersed into the α-CD, is yet only partially encapsulated in the case of α-TMCD (**1**): the iodine is located close to the center of the hydrophilic cavity, while the benzene ring, surrounded by the six glucose-3-OMe groups, is kept half outside with the amino group protruding therefrom. As there is also a water molecule included at the narrow end of the cavity that is hydrogen-bonded to a primary oxygen, it is obvious that packing effects resulting from solvation of the amino group also govern the orientation of the *p*-iodoaniline in α-TMCD (**1**), rather than hydrophobic effects only.

3 Conclusion

The interplay between various factors – polar interactions (host-guest complementarity of hydrophilic and lipophilic surface regions), crystal packing in the solid-state, solvation effects in (aqueous) solution, and enthalpy-entropy compensations – determines the orientation of the guest molecules inside the cyclodextrin cavities. Whereas the chiral resolution of enantiomers is relatively low for the unsubstituted CDs [18], the increased asymmetric cavity distortions in their per-*O*-alkylated derivatives seem to provide an enhanced ability to discriminate between enantiomeric guests [18]. Aside the operation of specific hydrogen bonding effects, the chiral recognition and the preferred inclusion of one enantiomer from a racemic mixture was proved to be also mediated by "induced-fit"-type changes of the macrocylic ring conformations, and by spatial fitting of apolar regions of the glucose residues with hydrophobic portions of the guest [18, 25].

The natural CDs exhibit a pronouncedly polar "poly-alcohol" type cavity which is able to accommodate even inorganic anions [30]. In contrast thereto, the "poly-ether"-type interior of the *O*-alkylated derivatives resembles more closely a crown-ether in terms of its functional groups and, hence, is able to act as a complexing agent for cations. Upon suitable exchange of some *O*-alkyl groups versus *O*-acyl residues, which support the incorporation of cations by providing additional complexing units, very strong hosts for metal ions in organic solvent are obtained, which in terms of their activity – not selectivity though – surpass even the crown-ethers [3].

By the way of summation, the essentially opposite lipophilicity profiles of cyclodextrins and their permethylated derivatives entail a different behavior towards inclusion complex formation, as borne out, for example, by the inverse incorporation of the very same guest into the cavities of α-CD and **1**, respectively, and by different depth of immersion. As this dis-

Table 1. Molecular Geometry Parameters and Cavity Characteristics of α-CD and β-CD in Comparison to their Permethylated Derivatives **1** and **2.**

Parameters[a]	Compounds:	α-CD	Per-*O*-methyl α-CD (**1**)	β-CD	Per-*O*-methyl β-CD (**2**)
Intersaccharidic torsion angles	$\langle\Phi\rangle$[b] [°]	108.1 (6.3)	103.7 (6.8)	111.9 (6.8)	103.9 (10.6)
	$\langle\Psi\rangle$[b] [°]	130.3 (7.6)	132.4 (11.0)	127.6 (8.0)	129.9 (17.3)
Bond angle	$\langle\gamma\rangle$[b] [°]	118.4 (2.0)	117.7 (2.7)	117.7 (2.6)	117.3 (3.0)
Tilt angle	$\langle\tau\rangle$[c] [°]	101.4 (5.9)	105.5 (9.8)	99.5 (7.1)	105.9 (15.7)
Cremer-Pople parameters	$\langle Q\rangle$ [Å]	0.57 (0.03)	0.58 (0.05)	0.58 (0.04)	0.58 (0.05)
	$\langle\theta\rangle$ [°]	5.5 (4.7)	6.6 (4.0)	5.0 (2.9)	6.2 (9.0)
	$\langle\phi\rangle$[d] [°]	118.7 (100)	118.5 (104)	173.5 (87)	197.4 (113.0)
Conformation		$^4C_1$	$^4C_1$	$^4C_1$	$^4C_1$
Torus diameter[e]	outer [Å]	14.2	14.5	15.7	16.5
	inner [Å]	5.2	4.2	6.6	5.8
Torus height[e]	[Å]	8.0	≈11.1	8.0	≈11.1
Surface area	total [Å^2]	720	970	845	1130
	cavity [Å^2]	85	120	105	180
Molecular volume	total [Å^3]	975	1400	1140	1645
	cavity [Å^3]	100	120	160	180

[a] A total of 42 different solid-state structures of α-CD with 51 crystallographically independent molecules were analyzed; per-*O*-methyl-α-CD (**1**): 11/11; β-CD: 48/59; per-*O*-methyl-β-CD (**2**): 13/13 geometries. – [b] Φ: O_5-C_1-O_1-$C_{4'}$; Ψ: C_1-O_1-$C_{4'}$-$C_{3'}$; φ: C_1-O_1-$C_{4'}$. – [c] angle between the least-squares best-fit mean plane of the macro rings (defined by all O-1 atoms) and each glucose-mean plane (atoms C_1 to C_5 and O_5). – [d] for $\theta \rightarrow 0.0°$ ($^4C_1$ conformations) the puckering angle ϕ and the corresponding root-mean-square (RMS) fluctuations become meaningless. – [e] effective molecular dimensions derived from the respective contact surfaces.

tinctively different behavior is mainly due to the opposite distribution of hydrophilic and hydrophobic surfaces areas in their cavities, the notion is substantiated that the operation of dispersive interactions between guest and host molecules play a more dominant role than hitherto appreciated.

4 Experimental

4.1 Molecular structures

All cyclodextrin structures and inclusion complex geometries were obtained from the Cambridge Crystallographic Data File (CCDF) [31], more recent structure determinations were included as long as the atomic coordinates had been provided. Hydrogen atoms not included in the molecular structures were positioned geometrically with standard bond lengths $r_{C\text{-}H}$=1.08Å and $r_{O\text{-}H}$=0.90Å, taking special care of possible intramolecular hydrogen bonding between neighbored hydroxyl groups. All given molecular parameters (cf. Table 1) discussed within this study had been recalculated from this data set. Structures of non- or mono-substituted cyclodextrins and their inclusion complexes on one hand side, and *per*-2,6-*O*- as well as *per*-2,3,6-*O*-substituted compounds on the other side were, analyzed separately by statistical methods (cf. Table 1).

The following structures of α-CD inclusion complexes had been used in Figure 2: α-CD *p*-iodoaniline trihydrate ($C_{36}H_{60}O_{30}\cdot C_6H_6IN\cdot 3H_2O$, CCDF-Refcode: CDEXIA01) [19a], 1·p-iodoaniline monohydrate ($C_{54}H_{96}O_{30}\cdot C_6H_6IN\cdot H_2O$, BEYLOG) [19b], α-CD·3-iodopropionic acid pentahydrate ($C_{36}H_{60}O_{30}\cdot C_3H_5IO_2\cdot 5H_2O$, BUPDEV) [20a], per-2,6-*O*-methyl-α-CD·3-iodopropionic acid ($C_{48}H_{84}O_{30}\cdot C_3H_5IO_2$, VERVET) [20b], α-CD·benzaldehyde hexahydrate ($C_{36}H_{60}O_{30}\cdot C_7H_6O\cdot 6H_2O$, BAJJAX) [21a], **1**·benzaldehyde ($C_{54}H_{96}O_{30}\cdot C_7H_6O$, BOHWUQ) [21b], α-CD·p-nitrophenol trihydrate ($C_{36}H_{60}O_{30}\cdot C_6H_5NO_3\cdot 3H_2O$, ACDPNP) [22a], and **1**·benzaldehyde monohydrate ($C_{54}H_{96}O_{30}\cdot C_6H_5NO_3\cdot H_2O$, BUDKEQ) [22b]; for clarity, water molecules of crystallization that are not included in the cyclodextrin cavities were removed. The per-*O*-methylated-α-CD (**1**) and β-CD units (**2**) were extracted from the iodoacetic acid monohydrate ($C_{54}H_{96}O_{30}\cdot C_2H_3IO_2\cdot H_2O$ BUPDIZ) [20a] and (S)-2-(2-fluor-biphen-4-yl)propionic acid ($C_{63}H_{112}O_{35}\cdot C_{15}H_{13}FO_2$, COYXET20) [25] inclusion complexes (Figure 3–5).

4.2 Molecular surfaces and Molecular Lipophilicity Patterns (MLPs)

Calculation of the molecular contact surfaces and the corresponding MLPs was carried out by using the MOLCAD [28, 29] molecular modeling program (Figures 4 and 5). Surfaces for the inclusion complexes were generated for the guest and host molecules separately, and were subsequently reassembled to the complex. Cross-cut plots perpendicular to the macrocycle and through the center of geometry were computed from the intersection of a plane with the molecular surfaces [32]; all black-and-white molecular plots were generated using the MolArch$^+$ program [32] (Figures 2 and 3). Visualization of the MLP surface qualities was done by color-coded projection of the computed values onto these surfaces by applying texture mapping [29b]. Scaling of the hydrophobicity patterns was performed in relative terms for each molecule separately, and no absolute values are displayed. Color graphics were photographed from the computer screen of a Silicon-Graphics workstation.

Acknowledgement

We thank Prof. Dr. *J. Brickmann*, Technische Hochschule Darmstadt, for providing us the MOLCAD molecular modelling software package.

Bibliography

[1] This account is Part 13 of the series "Molecular Modelling of Saccharides". – Part 12: *Lichtenthaler, F. W., P. Pokinskyj,* and *S. Immel:* Sucrose as a renewable organic raw material; New, selective entry reactions via computer simulation of its solution conformations and its hydroxyl group reactivities. Zuckerindustrie (Berlin) **120** (1996), 174–190.

[2] [2a] *Saenger, W.:* Cyclodextrin inclusion compounds in research and industry. Angew. Chem. **92** (1980), 343–361; Angew. Chem. Int. Ed. Engl. **19** (1980), 344–362. – [2b] *Saenger, W.:* Structural aspects of cyclodextrins and their inclusion complexes. In: Inclusion Compounds (J.L. Atwood, J.E.D. Davies, D.D. MacNicol, Eds.), Acad. Press, London, Vol. **2** (1984), pp. 231–259.

[3] *Wenz, G.:* Cyclodextrins as building blocks for supramolecular structures and functional units. Angew. Chem. **106** (1994), 85–870; Angew. Chem. Int. Ed. Engl. **33** (1994), 803–822.

[4] *Blokzijl, W.,* and *J. B. F. N. Engberts:* Hydrophobic effects, opinions and facts. Angew. Chem. **105** (1993), 1610–1624; Angew. Chem. Int. Ed. Engl. **32** (1993), 1545–1579.

[5] *Lichtenthaler, F. W.,* and *S. Immel:* Cyclodextrins, cyclomannins and cyclogalactins with five and six (1→4)-linked sugar units: comparative assessment of their conformations and hydrophobicity potential profiles. Tetrahedron Asymmetry **5** (1994), 2045–2060.

[6] *Lichtenthaler, F. W.,* and *S. Immel:* On the hydrophobic characteristics of cyclodextrins: computer-aided visualization of molecular lipophilicity patterns. Liebigs Ann. Chem. (1996), 27–37.

[7] *Lichtenthaler, F. W.,* and *S. Immel:* Towards understanding formation and stability of cyclodextrin inclusion complexes: computation and visualization of the lipophilicity patterns. Starch/Stärke **48** (1996), 145–154.

[8] *Croft, A.,* and *R. A. Bartsch:* Synthesis of chemically modified cyclodextrins. Tetrahedron **39** (1983), 1417–1474.

[9] *Mori, M., Y. Ito,* and *T. Ogawa:* A highly stereoselective synthesis of cyclomannohexaose (α-cyclomannin). Carbohydr. Res. **192** (1989), 131–146.

[10] *Fujita, K., H. Shimada, K. Ohta, Y. Nogami, K. Nasu,* and *T. Koga:* β-Cycloaltrin, a cyclooligosaccharide consisting of seven α(1→4)-linked altropyranones. Angew. Chem. **107** (1995), 1783–1784; Angew. Chem. Int. Ed. Engl. **34** (1995), 1621–1622.

[11] *Takeo, K., T. Sumitomo,* and *T. Kuge:* Improved synthesis of 6-deoxy analogs of cycloamyloses. Starch/Stärke **26** (1974), 111–118.

[12] *Gadelle, A.,* and *J. Defaye:* Selective halogenation at primary positions of cyclomaltooligosaccharides. Angew. Chem. **103** (1991), 94–96; Angew. Chem. Int. Ed. Engl. **30** (1991), 78–80.

[13] [13a] *Umezawa, S.,* and *K. Tatsuta:* Synthesis of amino derivatives of α-CD and of raffinose. Bull. Chem. Soc. Jpn. **41** (1968) 464–468. – [13b] *Tsujihara, K., H. Kurita,* and *M. Kawazu:* Highly selective sulfonylation of β-CD and synthesis of its pure amino derivatives. Bull. Chem. Soc. Jpn. **50** (1977), 1567–1571. – [13c] *Boger, J., R. J. Corcoran,* and *J. M. Lehn:* Selective modification of all primary hydroxyl group of α- and β-cyclodextrin. Helv. Chim. Acta **61** (1978), 2190–2218.

[14] *Parrot-Lopez, H., C. C. Ling, P. Zhang, A. Baszkin, G. Albrecht, C. de Rango,* and *A. W. Coleman:* Self-assembling systems of amphiphilic cationic per-6-amino-β-CD 2,3-di-*O*-alkyl ethers. J. Am. Chem. Soc. **114** (1992), 5479–5480.

[15] *Lindner, K.,* and *W. Saenger:* Crystal and molecular structure of β-CD dodecahydrate. Carbohydr. Res. **99** (1982), 103–115.

[16] [16a] *Nicolis, I., A. W. Coleman, P. Charpin, F. Villain, P. Zhang, C. C. Ling,* and *C. de Rango:* Molecular organization in the

6-bromo-6-deoxy-cyclodextrins. Formation of Molecular Layers. J. Am. Chem. Soc. **115** (1993), 11596–11597. – [16b] *Coleman, A. W., M. Munoz, H. Parrot-Lopez, P. Prognon, J.-M. Valleton, A. Baszkin, S. Alexandre, F. Sommer, T. Minh-Duc,* and *D. Wonessidjewe:* Tailoring cyclodextrins for the construction of large scale molecular assemblies. NATO ASI Series, Ser. C. **456** (1995), 77–97; Chem. Abstr. **123** (1995), 83863r.

[17] *Casu, B., M. Reggiani, G. G. Gallo,* and *A. Vigevani:* Conformation of *O*-methylated amyloses and cyclodextrins. Tetrahedron **24** (1968), 803–821.

[18] *Harata, K.:* Recent advances in the X-ray analysis of cyclodextrin complexes. In: Inclusion Compounds (J. L. Atwood, J. E. D. Davies, D. D. MacNicol, Eds.), Oxford Univ. Press, Oxford, UK, Vol. **5** (1991), pp. 311–344.

[19] [19a] *Saenger, W., K. Beyer,* and *P. C. Manor:* Topography of cyclodextrin inclusion complexes, VI. The crystal and molecular structure of α-cyclodextrin-p-iodoaniline trihydrate. Acta Crystallogr., Sect. B **32** (1976), 120–128. – [19b] *Harata, K., K. Uekama, M. Otagiri,* and *F. Hirayama:* The structure of the cyclodextrin complex, XI. Crystal structure of hexakis-(2,3,6-tri-*O*-methyl)-α-cyclodextrin p-iodoaniline monohydrate. Bull. Chem. Soc. Jpn. **55** (1982), 407–410.

[20] [20a] *Harata, K., K. Uekama, M. Otagiri,* and *F. Hirayama:* Crystal structures of α-cyclodextrin-3-iodopropionic acid (1:1) complex pentahydrate and hexakis(2,3,6-tri-O-methyl)-α-cyclodextrin iodoacetic acid (1:1) complex monohydrate. Nippon Kagaku Kaishi **1983**, 173–180; Chem. Abstr. **98** (1983), 135604 u. – [20b] *Harata, K.:* Crystal structure of the inclusion complex of hexakis-(2,6-di-*O*-methyl)-cyclomaltohexaose with 3-iodopropionic acid. Carbohydr. Res. **192** (1989), 33–42.

[21] [21a] *Harata, K., K. Uekama, M. Otagiri, F. Hirayama,* and *H. Ogino:* The structure of the cyclodextrin complex, X. Crystal structure of α-cyclodextrin benzaldehyde (1:1) complex hexahydrate. Bull. Chem. Soc. Jpn. **54** (1981), 1954–1959. – [21b] *Harata, K., K. Uekama, M. Otagiri, F. Hirayama,* and *Y. Sugiyama:* The structure of the cyclodextrin complex, XIV. Crystal structure of hexakis-(2,3,6-tri-*O*-methyl)-α-cyclodextrin benzaldehyde (1:1) complex. Bull. Chem. Soc. Jpn. **55** (1982), 3386–3389.

[22] [22a] *Harata, K.:* The structure of the cyclodextrin complex, V. Crystal structure of α-cyclodextrin complexes with p-nitrophenol and p-hydroxybenzoic acid. Bull. Chem. Soc. Jpn. **50** (1977), 1416–1424. – [22b] *Harata, K., K. Uekama, M. Otagiri,* and *F. Hirayama:* The structure of the cyclodextrin complex, XV. Crystal structure of hexakis-(2,3,6-tri-*O*-methyl)-α-cyclodextrin p-nitrophenol (1:1) complex monohydrate. Bull. Chem. Soc. Jpn. **55** (1982), 3904–3910.

[23] *Harata, K.:* Role of hydrogen bond and spatial fitting in the chiral recognition by cyclodextrins. J. Chem. Soc., Perkin Trans. 2 (1990), 799–804.

[24] *Schurig, V.,* and *H. P. Novotny:* Gaschromatographic separation of enantiomers on cyclodextrin derivatives. Angew. Chem. **102** (1990), 969–986; Angew. Chem. Int. Ed. Engl. **29** (1990), 939–958.

[25] *Harata, K., K. Uekama, T. Imai, F. Hirayama,* and *M. Otagiri:* Crystal structures of heptakis(2,3,6-tri-*O*-methyl)-β-cyclodextrin complexes with (*R*)- and (*S*)-fluorbiprofen. J. Incl. Phenom. **6** (1988), 443–460.

[26] *Yamamoto, Y., M. Onda, Y. Takahashi, Y. Inoue,* and *R. Chûjô:* Two-dimensional NMR spectra of *O*-methylated cyclodextrins. Carbohydr. Res. **170** (1987), 229–234.

[27] [27a] *Cremer, D.,* and *J. A. Pople:* A general definition of ring puckering coordinates. J. Am. Chem. Soc. **97** (1975), 1354–1358. – [27b] *Jeffrey, G. A.,* and *J. H. Yates:* Stereographic representation of the *Cremer-Pople* ring puckering parameters for pyranoid rings. Carbohydr. Res. **74** (1979), 319–322.

[28] [28a] *Brickmann, J.:* MOLCAD – MOLecular Computer Aided Design, Technische Hochschule Darmstadt, **1992**. The major part of the MOLCAD – program is included in the SYBYL package of TRIPOS Associates, St. Louis, USA. – [28b] *Brickmann, J.:* Molecular graphics – how to see a molecular scenario with the eyes of a molecule. J. Chim. Phys. **89** (1992), 1709–1721. – [28c] *Waldherr-Teschner, M., T. Goetze, W. Heiden, M. Knoblauch, H. Vollhardt,* and *J. Brickmann:* MOLCAD – Computer-aided visualization and manipulation of models in molecular science. In: Advances in Scientific Visualization (Eds.: F. H. Post, A. J. S. Hin), Springer, Heidelberg **1992**, pp. 58–67. – [28d] *Brickmann, J., T. Goetze, W. Heiden, G. Moeckel, S. Reiling, H. Vollhardt,* and *C.-D. Zachmann:* Interactive visualization of molecular scenarios with MOLCAD/SYBYL. In: Data Visualization in Molecular Science – Tools for Insight and Innovation (Ed.: J. E. Bowie), Addison-Wesley Publ., Reading, Mass. **1995**, pp. 83–97.

[29] [29a] *Heiden, W., G. Moeckel,* and *J. Brickmann:* A new approach to analysis and display of local lipophilicity/hydrophilicity mapped on molecular surfaces (MLP). J. Comput.-Aided Mol. Des. **7** (1993), 503–514. – [29b] *Teschner, M., C. Henn, H. Vollhardt, S. Reiling,* and *J. Brickmann:* Texture mapping, a new tool for molecular graphics. J. Mol. Graphics **12** (1994), 98–105.

[30] *Gelb, R. I., L. M. Schwartz, B. Cardelino, H. S. Fuhrmann, R. F. Johnson,* and *D. A. Laufer:* Cycloamylose complexation of inorganic ions. J. Phys. Chem. **87** (1983), 3349–3354.

[31] [31a] *Cambridge Crystallographic Data File,* Version 5.09, **1995**. – [31b] *Allen, F. H., S. A. Bellard, M. D. Brice, B. A. Cartwright, A. Doubleday, H. Higgs, T. Hummelink, B. G. Hummelink-Peters, O. Kennard, W. D. S. Motherwell, J. R. Rodgers,* and *D. G. Watson:* The Cambridge crystallographic data centre: computer-based search, retrieval, analysis, and display of information. Acta Crystallogr., Sect. B **35** (1979), 2331–2339. – [31c] *Allen, F. H., O. Kennard,* and *R. Taylor:* Systematic analysis of structural data as a research technique in organic chemistry. Acc. Chem. Res. **16** (1983), 146–153.

[32] *Immel, S., MolArch:* Molecular Architecture Modeling Program, Technical University of Darmstadt, **1996.**

Address of authors: Professor Dr. Dr. h.c. *Frieder W. Lichtenthaler* und Dr. *S. Immel.* Technische Hochschule Darmstadt, Institut für Organische Chemie. Petersenstraße 22, D-64287 Darmstadt (Germany).

(Received: March 28, 1996).